

ISI CORRELATIONS AND INFORMATION TRANSFER

MAURICE J. CHACRON, BENJAMIN LINDNER and ANDRÉ LONGTIN

*Department of Physics, University of Ottawa
150 Louis Pasteur, Ottawa, Ontario, K1N-6N5, Canada*

Received 9 January 2004

Revised 5 March 2004

Accepted 8 March 2004

Neurons produce action potentials or spikes in response to a wide variety of inputs. Correlations between interspike intervals are often seen in data from single neurons, and are due to a combination of intrinsic mechanisms and the temporal properties of the input stimulus. Here we review recent progress in our understanding of how intrinsic correlations arise in simple *biophysically* justified neuron models. We further describe the generic conditions under which these correlations enhance the rate of transfer of information about time-varying stimuli. This work points to the importance of studying non-renewal first passage time problems in nonlinear dynamical systems.

Keywords: Excitable systems; neurons; correlations; non-renewal processes; information theory; integrate-and-fire.

1. Introduction

Excitable systems generate spikes when one or more of their state variables enter a certain region of phase space. The correlations between such temporally localized spikes, or between quantities derived from spike trains such as interspike interval sequences, are under scrutiny in a wide range of disciplines (see e.g. the recent review in [1]), namely in the biological sciences where interest in heart rate and neural variability is high. The study of the genesis of and interplay between short and long range correlations is likely to be a challenging and fruitful area of research for many years to come.

From the deterministic point of view, it is not surprising that correlations between interspike intervals (ISIs) exist in neurons. This is obvious e.g. in the autonomous behavior known as bursting. It is also obvious when a neuron is forced periodically and displays anything but $n:n$ phase locked firing (n spikes in response to n forcing cycles). For example, a 1:2 pattern has two intervals, and this sequence of intervals is periodic and therefore has a periodic autocorrelation. Underlying this correlation is a memory of previous activity prior to the spike, i.e. the occurrence

of the spike does not reset all the state variables to some standard location in phase space.

In the presence of noise, one typically wants to calculate the mean first passage time to threshold. This is usually a complex task, one that can only be done with approximations except for the simplest models, even though its basic assumption is that one is dealing with a renewal point process: each realization to threshold starts from the same location, independently of how long it took to get to threshold on the previous interval. Correlations imply memory that carry over after a spike, and it is not obvious how to introduce that fact into calculations.

Modeling the presence of correlations can provide useful insights into the biophysical properties of cells. Further, they can point to interesting functional roles for correlations. An understanding of the origins of correlations and of their potential effects on information transfer is only beginning to emerge. In this paper, we summarize some of our contributions on this issue. It is not surprising that correlated intervals can arise in response to time varying stimuli; the stimuli leave a footprint of their correlations on the interval sequence. Here however, we concentrate on the correlations that arise from the intrinsic behavior of the cell, i.e. that exists even in the absence of forcing. The correlating mechanisms may then interact with specific input properties, as we will see.

Our review is organized as follows. We first present experimental data from weakly electric fish electroreceptor neurons displaying correlated interspike intervals. A biophysically justified model is then presented that reproduces these correlations and numerical simulations reveal that their presence can increase information transfer. Observations of noise shaping in the power spectrum then lead us to formulation of simpler and more abstract models where we show theoretically how correlations shape the spike train power spectrum in a way that enhances information transfer.

2. Electoreception in Weakly Electric Fish

Weakly electric fish use modulations of their self-generated electric field to locate prey and communicate with conspecifics [2]. Electroreceptor neurons located on their skin are sensitive to amplitude modulations of the quasi-sinusoidal electric organ discharge (EOD) generated by the animal [3]. Experimental recordings from electroreceptor neurons display noisy phase-locking to the EOD [4–7]. Figure 1a shows the interspike interval histogram (ISIH) from such an electroreceptor neuron. The ISIH displays Gaussian shaped modes near integer multiples of the EOD cycle. These neurons thus skip an apparently random number of EOD cycles between firings due to significant amounts of noise. A review of dynamical mechanisms that give rise to such skipped firings can be found in [8]. However, these electroreceptors display non-renewal ISI statistics due to a prominent negative ISI serial correlation coefficient (SCC) at lag one. These SCC's are defined as:

$$\rho_j = \frac{\langle (I_{i+j} - \langle I_i \rangle) (I_i - \langle I_i \rangle) \rangle}{\langle (I_i - \langle I_i \rangle)^2 \rangle} \quad (1)$$

where $\{I_i\}$ denotes the ISI sequence, j is the lag, and the average $\langle \dots \rangle$ is performed over index i .

There is much variability in firing rate and ISIH shape across different electroreceptor units [9, 10]. However, for a given electroreceptor, these quantities are

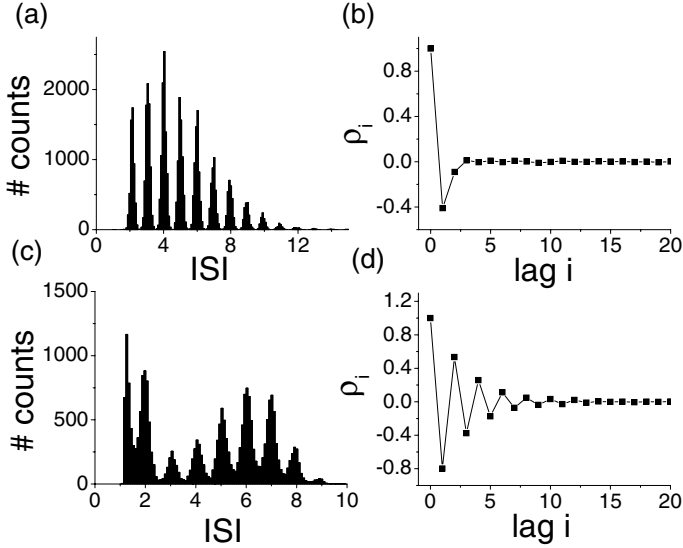


Fig. 1. (a) ISIH from a non-bursting electroreceptor. The multi-modal structure results from phase-locking to the EOD. Note that ISIs are expressed as multiples of the EOD cycle. (b) ISI serial correlation coefficients from this unit showing a negative value at lag one. (c) ISIH from a bursting electroreceptor. Note the bimodal envelope and that the ISIs are expressed in multiples of the EOD cycle. (d) ISI serial correlation coefficients from this electroreceptor showing temporal anti-correlations similar to other types of electroreceptors. 21000 and 23924 consecutive ISIs were analyzed for the non-bursting and bursting units, respectively. The EOD frequency was 885 Hz and 905 Hz for the non-bursting and bursting units, respectively. Data courtesy of L. Maler (University of Ottawa).

very stable and reproducible. Electroreceptors have been characterized to be either bursting or non-bursting depending on the fraction of action potentials fired on consecutive EOD cycles. Some electroreceptors tend to fire packets of action potentials (bursts) and this is manifested in the ISIH by a prominent peak at one EOD cycle. Fig. 1c shows the ISIH from one such unit. The envelope is bimodal as expected for bursting neurons. Fig. 1d shows the ISI SCC's for this bursting unit. Instead of just one negative SCC at lag one like for the non-bursting unit, this unit displays anti-correlations that decay over a few lags. These ISI anti-correlations are similar to those seen in other types of electroreceptors [11] that can also exhibit bursting dynamics [12].

3. Modeling Electroreceptor Dynamics

It was found that electroreceptor neurons could be modeled with a simple variant of the leaky integrate and fire (LIF) model: the leaky integrate and fire with dynamic threshold (LIFDT) model [4–6]:

$$\dot{v} = -\frac{v}{\tau_v} + I_{syn} \quad (2)$$

$$\dot{w} = H(t - t_{last} - T_r) \left(\frac{w_0 - w}{\tau_w} \right) + \Delta w \delta(t - t_{last}) \quad (3)$$

where v is the membrane voltage, w is the threshold, T_r is the absolute refractory period, and I_{syn} is the synaptic current. We let the threshold carry the memory by the following firing rule: when $v = w$, v is reset to zero as in a standard LIF model, while threshold is incremented by a constant amount Δw and kept constant for the duration of the absolute refractory period T_r ; after this time T , the threshold relaxes exponentially towards its equilibrium value w_0 until the next spiking time. If two spiking times occur within close proximity of one another, the threshold will cumulatively increase leading to greater refractoriness. Thus, a short ISI will tend to be followed by a long one and the model displays negative ISI correlations [13] as in the experimental data for the non-bursting electroreceptor [4]. With a minor modification (a facilitating current driven by spiking), the model is capable of reproducing the bursting dynamics displayed by some electroreceptors [5, 7].

4. Effects of ISI Correlations on Information Transfer

Another model, which we refer to as the Nelson model, has been proposed earlier for electroreceptor neurons [9]. A detailed comparison study between the Nelson model and the LIFDT model found that both displayed similar dynamics except that the Nelson model did not display any significant ISI correlations [6]. Comparing the Nelson and LIFDT models should then give one insight on the effects of ISI correlations on signal transmission. Information theory was originally developed by Shannon [14] in the context of communication systems. It has been adapted to provide a measure of the information encoding capacity of neurons [15]. Spike trains from electroreceptor neurons are noisy since they display high entropy [6, 16].

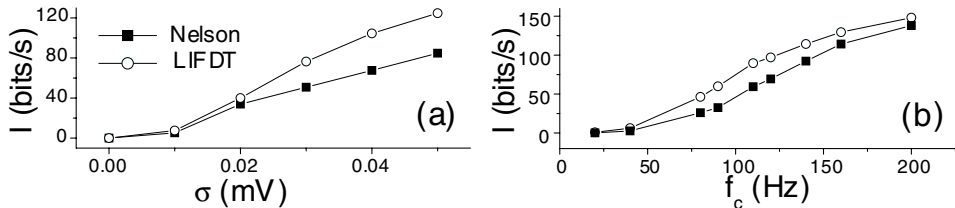


Fig. 2. (a) Mutual information rate I as a function of stimulus contrast σ for the LIFDT (open symbols) and Nelson (filled symbols) models. (b) Mutual information rate I as a function of stimulus cutoff frequency f_c . In both cases, the stimulus was low-passed filtered Gaussian white noise with cutoff frequency f_c and standard deviation σ . The mutual information rate is higher for the LIFDT model than for the Nelson model due to negative ISI correlations.

Figure 2a shows the information transmission rates for the LIFDT and Nelson models. It is seen that the rate of information transmission is greater for the LIFDT model over a broad range of stimulus contrasts and temporal frequency content. Other results [6, 17] using signal detection theory [18] show that negative ISI correlations reduce the variance of the spike count over a given time interval, allowing better signal detectability. On the other hand, positive ISI correlations will increase spike train variability. Other results show that an interaction between short-range negative ISI correlations and long-range positive ISI correlations can create a time window where spike train variability is minimal [6, 19].

5. The Mechanism: Reduction of Noise Power at Low Frequencies

In this section, we explore the actual mechanism by which negative ISI correlations increase information transfer. Figure 3 shows the spike train power spectra from the LIFDT and Nelson models for baseline activity (i.e. no stimulus). It is observed that the LIFDT model has weaker power at low frequencies than the Nelson model.

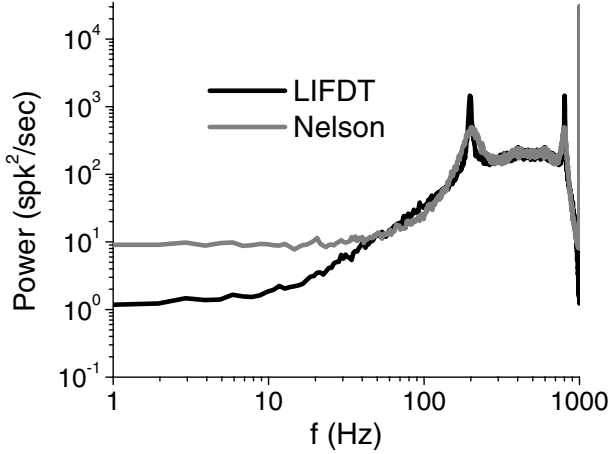


Fig. 3. Spike train power spectra for the LIFDT (black) and Nelson models (gray). The LIFDT model has lower power at low frequencies due to negative ISI SCC's (see text). The peak at 200 Hz corresponds to the afferent's intrinsic firing rate while the peak at 1000 Hz corresponds to the EOD forcing. There is a peak at 800 Hz due to interactions between the two oscillations.

This can be understood from the following formula [20]:

$$\lim_{f \rightarrow 0} P(f) = \mu CV^2 \left(1 + 2 \sum_{i=1}^{\infty} \rho_i \right) \quad (4)$$

where CV is the standard deviation to mean ratio of the ISI distribution and μ is the mean firing rate. As both CV and μ are virtually equal for the LIFDT and Nelson models [6], the low frequency power only differs due to the ISI SCC's: the negative SCC at lag one for the LIFDT model reduces noise power at low frequencies. Note also that the electroreceptor neuron has its own intrinsic firing frequency causing a peak around 200 Hz. It is also periodically forced by the EOD at 1000 Hz. There are also peaks at 800 Hz and 1200 Hz as expected for nonlinear interactions between two limit cycles. In other types of electroreceptors, this forcing is achieved via intrinsic hair cell oscillations but the power spectra have a similar shape [21].

For a further understanding of the baseline activity with negative ISI correlations and its effect on the signal transmission performance, we recently constructed two simplified neuron models that allow for an analytical treatment of the information transfer characteristics [23]. These two models have the same statistics for a single ISI distribution and identical linear response with respect to sinusoidal current stimulation. This approach is similar to that used above in our comparison of the Nelson and LIFDT models, although in that case, the similarity was not exact; parameters were adjusted to give similar numerical values of firing rates and similar

ISIH's. Like the latter ones, the simplified models differ in their ISI correlations: the spike train of model A will display strong negative correlations like the LIFDT model whereas model B generates a renewal spike train like the Nelson model. Therefore we can expose the effect of correlations on the information transfer.

We consider a *perfect* IF model governed by the simple differential equation

$$\dot{v} = \mu + s(t) \quad (5)$$

where μ denotes the base current on which we superimpose the signal current $s(t)$ where time is now dimensionless for generality. Note that a leakage term, a periodic modulation, and an internal noise current as they were used in the LIFDT model are absent in Eq. (5). Both reset rules are illustrated in Fig. 4.

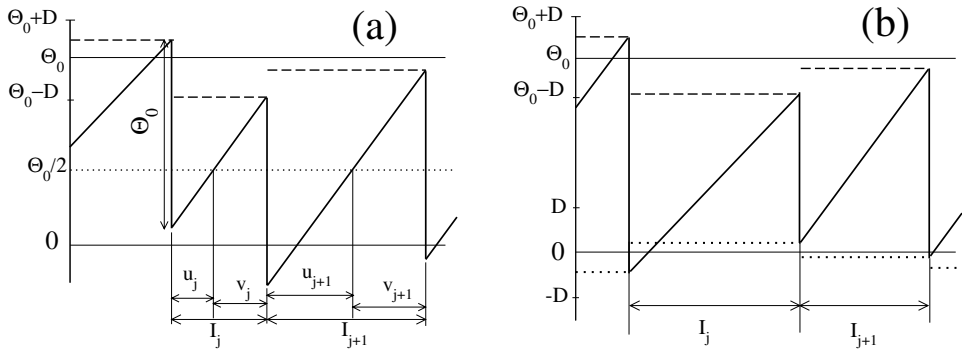


Fig. 4. Illustration of simplified models. *Left:* Model A for $s(t) \equiv 0$. In between action potentials the voltage $v(t)$ (solid line) evolves according to Eq. (5). A threshold value (shown by the dashed line) has been drawn from the uniform density $[\Theta_0 - D, \Theta_0 + D]$ the boundaries of which are indicated. Once the voltage hits the threshold, a spike is fired and v is decremented by Θ_0 . Each ISI I_j consists of two sub-intervals u_j and v_j that are defined as the passage times from reset to $\Theta_0/2$ (dotted line) and from the latter point to the threshold, respectively. *Right:* Model B for $s(t) \equiv 0$. In this case, threshold values (dashed line) and reset values are drawn from uniform densities the boundaries of which are indicated. Note that both random values (drawn after each firing) are independent of each other in marked contrast to model A. A subdivision of the indicated intervals as for model A is also possible but has here been omitted for the sake of clarity of the illustration.

We introduce an internal noise by randomization of the threshold and reset voltage values. The threshold value is drawn from a uniform density $[\Theta_0 - D, \Theta_0 + D]$ with $D < \Theta_0/2$; each time the threshold is reached by the voltage variable a spike is fired and we draw another value, which is entirely independent from the previous values of the threshold. Such a randomization of the threshold will obviously lead to a stochastic spike train; it has been used previously (see e.g. Ref. [22]) as an alternative model that is easier to tackle analytically than IF models with noisy input currents.

The crucial point in the further construction of the two models is the way in which the voltage variable is reset after firing. For model A we choose the following reset rule: after generation of a spike, the voltage is *decremented* by the constant value Θ_0 . This will lead to a randomization of the reset point which will be uniformly distributed in the interval $[-D, D]$. Note however that the reset point is entirely

correlated with the previous value of the threshold. For model B in contrast, we reset the voltage to a value uniformly distributed in the interval $[-D, D]$ independently of previous values of both threshold and reset points. Parameters are, here and in the following: $\mu = 1$, $\Theta_0 = 1$, and $D = 0.2$.

We consider first the spontaneous activity ($s(t) \equiv 0$) which is crucial for the signal transmission features of the two models. For both models each ISI I_j can be split into two sub-intervals u_j and v_j which are defined by the passage times from reset value to $\Theta_0/2$ and from $\Theta_0/2$ to the current value of the threshold (the subintervals are indicated in Fig. 4a). Both u_j and v_j are uniformly distributed in the intervals $[(\Theta_0/2 - D)/\mu, \Theta_0/2 + D)/\mu]$. The ISI density is then given by the convolution of these two random variables which yields a triangular distribution.

For model A, because of the reset rule, it is easily seen that $v_j + u_{j+1} = \Theta_0/\mu$ (within these two sub-intervals, the voltage passes exactly the distance Θ_0 by which it is decremented after firing). Using this relation together with the mutual independence of u_j, v_{j+1} , and u_{j+1} , a little calculation reveals that $\rho_1 = -0.5$ while the SCC at higher lags is zero. This is qualitatively the same as observed in the LIFDT model with parameters that reproduce the experimental data (cf. Fig. 1): a strong negative correlation between subsequent ISIs and very weak correlations between ISIs that are further apart of each other. For model B, we obtain obviously a renewal spike train since the interval I_j is uniquely determined by the reset and threshold value that are independent of previous reset and threshold values and thus of previous ISIs.

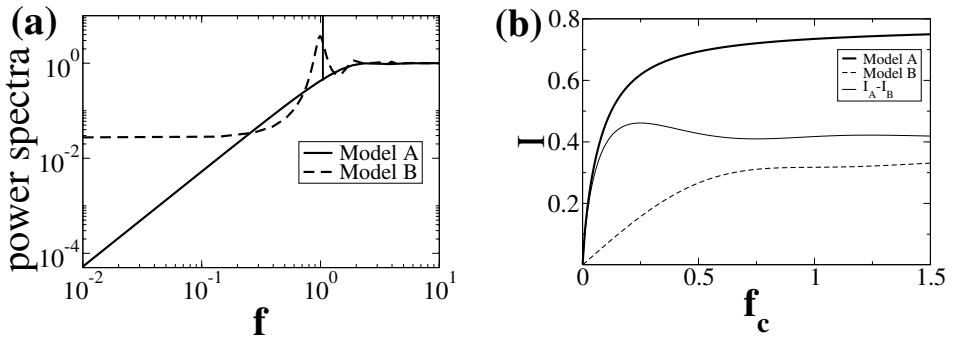


Fig. 5. *Left*: Power spectra for the spike trains of the simplified models and $s(t) \equiv 0$. *Right*: Mutual information for models A and B (solid and dashed lines) vs cut-off frequency f_c ($\alpha = 0.0156$); also shown is the difference between these functions (thin solid line).

Analytical formulas for the power spectra of the baseline activity ($s(t) \equiv 0$) can be calculated; we refer to Ref. [23]. In Fig. 5 we show the power spectra for both models in the spontaneous case ($s(t) \equiv 0$). Two distinct features can be observed in qualitative agreement with the power spectra for LIFDT and Nelson models in Fig. 3: (1) the negative correlations lead to a suppression of power at low frequencies for model A; (2) the peak at the eigenfrequency is sharper for model A (note the δ peak at $f = 1$ indicated by a line). Due to the simplicity of our model, both features are overdrawn: since $\rho_1 = -0.5$ for model A the power spectrum goes to zero in the zero-frequency limit; further, for the same reason, the spike train of model A

shows a “never-ending” oscillation which becomes manifest by a δ spike instead of a peak with small but finite width as for the LIFDT model. However, the main effect of the negative correlations is for both model A and the LIFDT model the same, namely, a “noise shaping”, i.e. a shift of spectral power from low frequencies to higher frequencies (the total power is not changed).

Why does the noise shaping of the baseline activity lead to an enhanced information transfer of an additional signal $s(t)$? Any information transfer will be distorted by the internal noise present in the neural spike train. This internal noise is - at least for a weak external stimulation — given by the baseline activity, i.e. the power spectra shown in Fig. 5a will be the background spectra if the transmission of a finite signal $s(t)$ is considered. A significant lowering of the background spectrum in the low frequency range implies that within this frequency range the information transmission will be increased. Obviously, in a certain higher frequency range the transmission will be decreased. If the stimulus $s(t)$ is a band-limited white noise, the overall effect of the noise shaping and thus of the negative correlations in the ISI sequence is an increase in information transmission. This is shown in Fig. 5b for the mutual information as a function of the cut-off frequency of the stimulus which was Gaussian noise with uniform spectral density $S(f) = \alpha$ for $\alpha < f_c$ and zero beyond the cut-off frequency f_c . Clearly, the mutual information for model A is much higher than for model B for all cut-off frequencies. For general stimuli with arbitrary power spectrum, we expect that negative correlations will enhance information transmission through noise shaping. Although it is possible to construct an input spectrum for which the mutual information is *lower* for the non-renewal model A (e.g. an input spectrum that is sharply peaked in the range where the background spectrum of the renewal model is lower), such narrow bandpass input would be rather particular; it would have to be adjusted knowing the parameters of the internal dynamics of the neuron. Finally we note that the difference between the transmitted information of both systems (thin solid line in Fig. 5b) shows a maximum at a finite cut-off frequency. This is again a feature also found in the LIFDT model, but not in the Nelson model (cf. Ref. [5]). The results as a function of f_c here and in [5] are not computed under precisely the same conditions; total power is constant in [5], but both effects probably have a common origin, a connection that will be explored elsewhere.

The simplified models discussed here show that noise shaping by negative correlations is the mechanism for the enhancement of signal transmission. It is important to note that many details of the LIFDT model which were needed to reproduce the experimental data from the P-units of the weakly electric fish are not needed to see the effect of an transmission enhancement. Most of the external and internal time scales present in the detailed LIFDT model (EOD frequency, correlation times of internal colored noise sources, leakage term of the LIF model, etc.) can be removed: a perfect IF model with threshold noise and a reset rule that provides a source of memory in the ISI sequence suffice to observe the basic effect.

6. Discussion

We have reviewed recent results concerning the origin of intrinsic correlations between firing intervals in excitable systems, and their influence on the information

transfer characteristics. Many neurons like weakly electric fish electroreceptors display intrinsic correlations. Many ion channels can give rise to ISI correlations and the effects of these are qualitatively similar to our model with dynamic threshold [24]. Our dynamic threshold can further model other phenomena such as lateral inhibition and synaptic depression [13]. Our biophysically justified LIFDT model can reproduce the ISI correlations seen experimentally [4, 7].

Numerical simulations comparing the LIFDT model to a previous renewal model proposed by Nelson and coworkers [9] have revealed that negative ISI correlations could increase information transfer and signal detectability [5, 7, 17]. Comparing the power spectra of the LIFDT and Nelson models revealed that negative ISI correlations could decrease the power at low frequencies.

This observation lead us to construct simple models where analytical calculations are possible. Our theoretical results revealed the mechanism by which ISI correlations can increase information transfer: shaping of the noise power spectrum. In particular, negative ISI correlations decrease the noise power at low frequencies thereby increasing information transfer of stimuli containing these frequencies.

Although such correlations are often characterized experimentally, they raise serious complications from the theoretical point of view in the absence of noise, as well as in its presence. Deterministically, correlations can give rise to adaptation and complex phase locked dynamics and even chaos [13, 25]. In the context of noise, the mean first passage time to threshold calculations are complicated by the non-renewal property, and new tricks have to be devised [23].

Possible future directions include investigating (theoretically and numerically) the same effects of correlations as shown here in more realistic leaky (i.e. non-perfect) integrate and fire neurons, or even type I neurons with saddle-node dynamics. This may reveal new effects and even new benefits due to correlations. Because the effect of correlations seem to be enhanced for a given frequency content of the input signal, we anticipate that certain time scale matching conditions may exist between correlations and input. Further, it is important to eventually develop the theory for positive correlations as well as for mixes of positive and negative correlations. Our numerical studies have found in fact that the combination of these two kinds of correlations can set time scales over which spike train variability has optimal properties, as displayed e.g. by Fano factors. Theoretical insight into such problems is thus needed. Finally, it will be interesting to see whether correlations enhance information transfer properties by noise shaping in other non-neural systems, and whether they can even be added artificially for that purpose.

Acknowledgements

We would like to thank L. Maler for useful discussions and for sharing his data with us. This research was supported by NSERC Canada and the Ontario Premier's Research Excellence Award program (AL).

References

- [1] Processes with long-range correlations: Theory and Applications, ed. by G. Rangarajan and M. Ding, Springer, Berlin (2003).

- [2] R. W. Turner, L. Maler and M. Burrows, *Electroreception and electrocommunication*, Company of Biologists, Cambridge, UK (1999) 1167–1458.
- [3] J. Bastian, *Electrolocation I. How the electroreceptors of Apterontus Albifrons code for moving objects and other electrical stimuli*, *J. Comp. Physiol. A* **144** (1981) 481–494.
- [4] M. J. Chacron, A. Longtin, M. St-Hilaire and L. Maler, *Suprathreshold stochastic firing dynamics with memory in P-type electroreceptors*, *Phys. Rev. Lett.* **85** (2000) 1576–1579.
- [5] M. J. Chacron, A. Longtin and L. Maler, *Simple models of bursting and non-bursting P-type electroreceptors*, *Neurocomputing* **38** (2001) 129–139.
- [6] M. J. Chacron, A. Longtin and L. Maler, *Negative interspike interval correlations increase the neuronal capacity for encoding time-dependent stimuli*, *J. Neurosci.* **21** (2001) 5328–5343.
- [7] M. J. Chacron, *Neural Dynamics leading to Optimized Information Transfer*, Ph. D. Thesis, University of Ottawa (2003).
- [8] A. Longtin, *Phase locking and resonances for stochastic excitable systems*, *Fluct. Noise Lett.* **2** (2002) 183–203.
- [9] M. E. Nelson, Z. Xu and J. R. Payne, *Characterization and modeling of P-type electrosensory afferent responses to amplitude modulations in a wave-type electric fish*, *J. Comp. Physiol A* **181** (1997) 532–544.
- [10] R. Ratnam and M. E. Nelson, *Non-renewal statistics of electrosensory afferent spike trains: implications for the detection of weak sensory signals*, *J. Neurosci.* **20** (2000) 6672–6683.
- [11] S. Bahar, J. W. Kantelhardt, A. Neiman, H. H. A. Rego, D. F. Russell, L. Wilkens, A. Bunde and F. Moss, *Long-Range temporal anti-correlations in paddlefish electroreceptors*, *Europhys. Lett.* **56** (2001) 454–460.
- [12] A. Neiman and D. F. Russell, *Synchronization of noise-induced bursts in noncoupled sensory neurons*, *Phys. Rev. Lett.* **88** (2002) 138103.
- [13] M. J. Chacron, K. Pakdaman and A. Longtin, *Interspike interval correlations, memory, adaptation, and refractoriness in a leaky integrate-and-fire model with threshold fatigue*, *Neural Comp.* **15** (2003) 253–278.
- [14] C. E. Shannon, *The mathematical theory of communication*, *Bell Systems Technical Journal* **27** (1948) 379–423.
- [15] A. Borst and F. E. Theunissen, *Information theory and neural coding*, *Nature Neuroscience* **2** (1999) 947–957.
- [16] R. Steuer, W. Ebeling, D. F. Russell, S. Bahar, A. Neiman and F. Moss, *Entropy and local uncertainty of data from sensory neurons*, *Phys. Rev. E* **64** (2001) 061911.
- [17] A. Longtin, C. Laing and M. J. Chacron, *Correlation and memory in neurodynamical systems*, in *Processes with long-range correlations: Theory and Applications*, ed. G. Rangarajan and M. Ding, Springer, Berlin (2003) 286–308.
- [18] D. Green and J. Swets, *Signal Detection Theory and Psychophysics*, Wiley, New York (1966).
- [19] J. W. Middleton, M. J. Chacron, B. Lindner and A. Longtin, *Firing statistics of a neuron driven by long-range correlated noise*, *Phys. Rev. E* **68** (2003) 021920.
- [20] D. R. Cox and P. A. W. Lewis, *The Statistical Analysis of Series of Events*, Methuen, London (1966).
- [21] A. Neiman and D. F. Russell, *Stochastic biperiodic oscillations in the electroreceptors of paddlefish*, *Phys. Rev. Lett.* **86** (2001) 3443–3446.

- [22] G. Gestri, H. A. K. Masterbroek and W. H. Zaagman, *Biol. Cybern.* **38**, 31 (1980).
- [23] M.J. Chacron, B. Lindner and A. Longtin, *Noise shaping by interval correlations increases information transfer*, *Phys. Rev. Lett.* **92** (2004) 080601.
- [24] Y. H. Liu and X. J. Wang, *Spike Frequency adaptation of a generalized leaky integrate-and-fire neuron*, *J. Comp. Neurosci.* **10** (2001) 25–45.
- [25] M. J. Chacron, A. Longtin and K. Pakdaman, *Chaotic Firing in the Sinusoidally Forced Leaky Integrate-and-Fire Model with Threshold Fatigue*, *Physica D* (in press).